

OFF-AXIS VISCOPLASTIC BEHAVIOR OF PLAIN-WOVEN LAMINATES: ANALYSIS USING TIME-DEPENDENT HOMOGENIZATION THEORY

Keisuke Nakata*, Tetsuya Matsuda*, Masamichi Kawai*

*Department of Engineering Mechanics and Energy, University of Tsukuba

Keywords: *plain-woven laminate, homogenization, off-axis, viscoplastic, creep*

Abstract

In this study, the off-axis elastic-viscoplastic and creep behaviors of plain-woven GFRP laminates are analyzed by using a homogenization theory. First, the point-symmetry of the internal structures of plain-woven laminates is utilized for the boundary condition of unit cell problems, reducing the domain of analysis to 1/4 and 1/8 for the in-phase and out-of-phase laminate configurations, respectively. The time-dependent homogenization theory is then developed for the reduced domain of analysis. Using the present method, the in-plane elastic-viscoplastic and creep deformations of plain-woven glass fiber/epoxy laminates are analyzed. Moreover, the in-plane uniaxial tensile tests of a plain-woven GFRP laminate at a constant strain rate are performed at a room temperature. It is thus shown that the present analysis successfully predicts the in-plane elastic-viscoplastic behavior of plain-woven GFRP laminates. It is also shown that the laminates exhibit marked in-plane anisotropy with respect to the elastic-viscoplastic and creep behaviors.

1 Introduction

It is of great importance to analyze the mechanical properties of textile composites because of their wide use in major industrial sectors, such as aerospace, auto and marine industries (e.g., [1,2]). Especially, plain-woven laminates made of plain fabrics and polymer matrix materials are regarded as the most fundamental textile composites. Thus, many studies have focused on analytical or numerical approaches to predict the mechanical properties of plain-woven laminates [1]. Early works drew attention to the linear elastic properties of laminates (e.g., [3-5]). But, recently, more attention

is paid to the nonlinear analysis of plain-woven laminates because laminates generally exhibit nonlinear behavior due to the inelastic deformation of matrix materials or the microscopic failures of fibers and matrix (e.g., [6-10]).

To predict such nonlinear behavior of plain-woven laminates, numerical approaches are advantageous because they have the capability of analyzing the microscopic distributions of stress and strain in laminates, i.e., microscopic information providing accurate nonlinear analysis in incremental form. The mathematical homogenization theory based on a unit cell problem [11-13] is one of the most useful theories for such numerical analysis of plain-woven laminates because the theory enables us to analyze the microscopic stress and strain distributions as well as the macroscopic behavior of laminates. The theory, therefore, has been already applied to the microscopic failure propagation analysis of plain-woven GFRP laminates subjected to in-plane on-axis load [8,14,15]. Another numerical approach, finite element analysis, was also successfully applied to the same kind of failure propagation analysis of plain-woven laminates [7,10,16,17].

In the previous papers [18,19], the authors have developed the homogenization theory for nonlinear time-dependent composites, which will be referred to as the time-dependent homogenization theory hereafter. The theory was then applied to analyzing the elastic-viscoplastic behavior of long fiber-reinforced laminates, and succeeded in predicting experimental results accurately [20,21]. Using the theory, therefore, we may be able to analyze the off-axis nonlinear time-dependent behavior of plain-woven laminates. Such an analysis, however, has been hardly reported so far.

The present authors [21,22] further showed the following: If the internal structure of a composite has point-symmetry, the perturbed velocity field in

the composite also has point-symmetry. Using the point-symmetry of perturbed velocity field as a boundary condition of unit cell problems, we are able to reduce the domain of analysis, leading to considerable computational efficiency. In the homogenization analysis of plain-woven laminates, the internal structures of the laminates are generally assumed to have the point-symmetry as well as the Y -periodicity. Thus, the point-symmetric boundary condition can be introduced into the homogenization analysis of plain-woven laminates so that the domain of analysis can be reduced. But, so far, whole unit cells have been taken as the domain of analysis because of the restriction of the Y -periodic boundary condition [4,8,14,15].

In this study, we analyze the in-plane off-axis elastic-viscoplastic and creep deformations of plain-woven GFRP laminates using the time-dependent homogenization theory. It is first shown that, assuming the in-phase and out-of-phase laminate configurations of plain fabrics in laminates, both the internal structures have point-symmetry. It is further shown that the use of point-symmetry as a boundary condition for boundary value problems allows part

of the unit cells for the domain of analysis. The time-dependent homogenization theory is then reconstructed for the reduced domain of analysis. The present method is next applied to the analysis of the in-plane elastic-viscoplastic and creep behaviors of plain-woven GFRP laminates. Moreover, tensile tests of a plain-woven GFRP laminate at a constant strain rate are carried out to compare the results of experiments with those of the present analysis.

2 Domain of Analysis

In the homogenization analysis of plain-woven laminates, two patterns of laminate configurations of plain fabrics, i.e., the in-phase and out-of-phase laminate configurations, are generally employed as the internal structures of plain-woven laminates as mentioned in the previous section [4,8,14,15]. The in-phase laminate configuration has no offset of plain fabrics in the y_1 - and y_2 -directions (Fig. 1(a)), while the out-of-phase laminate configuration has the phase shift of plain fabrics by π in the y_1 - and y_2 -directions (Fig. 1(b)). According to the previous studies [4,8,14,15], the assumption of these laminate configurations provides fairly valid results, although the actual microstructures of plain-woven laminates are not perfectly periodic but random to a greater or less extent. In this section, therefore, we also take the two laminate configurations into consideration, and show that the plain-woven laminates with such configurations have point-symmetric internal structures. It is further shown that the point-symmetry is able to be utilized as a boundary condition for boundary value problems so that we can reduce the domain of analysis. Incidentally, the influence of the misalignment of plain fabrics or the nesting of fiber bundles on the mechanical properties of plain-woven laminates can be found in the literature [17,23-25].

First, with an in-phase laminate configuration, a unit cell Y of laminate is taken as shown by the dashed lines in Fig. 2(a). Now, we turn our attention to a part of Y , which is indicated by the solid lines in Fig. 2(a) and referred to as a basic cell A hereafter. A careful look at the figure reveals that the internal structure of laminate has point-symmetry with respect to the centers of lateral facets of A , which are denoted by the open circles in Fig. 2(a). The perturbed velocity in laminate, therefore, distributes point-symmetrically with respect to these points. By contrast, the perturbed velocity at the top and bottom facets of A satisfies the Y -periodicity because the internal structure is periodic with respect

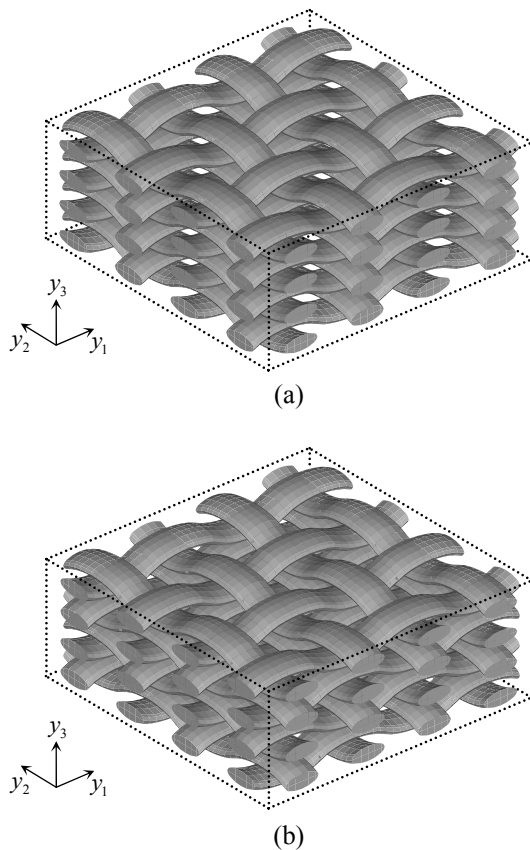


Fig. 1. Two types of laminate configurations of plain fabrics; (a) in-phase, (b) out-of-phase.

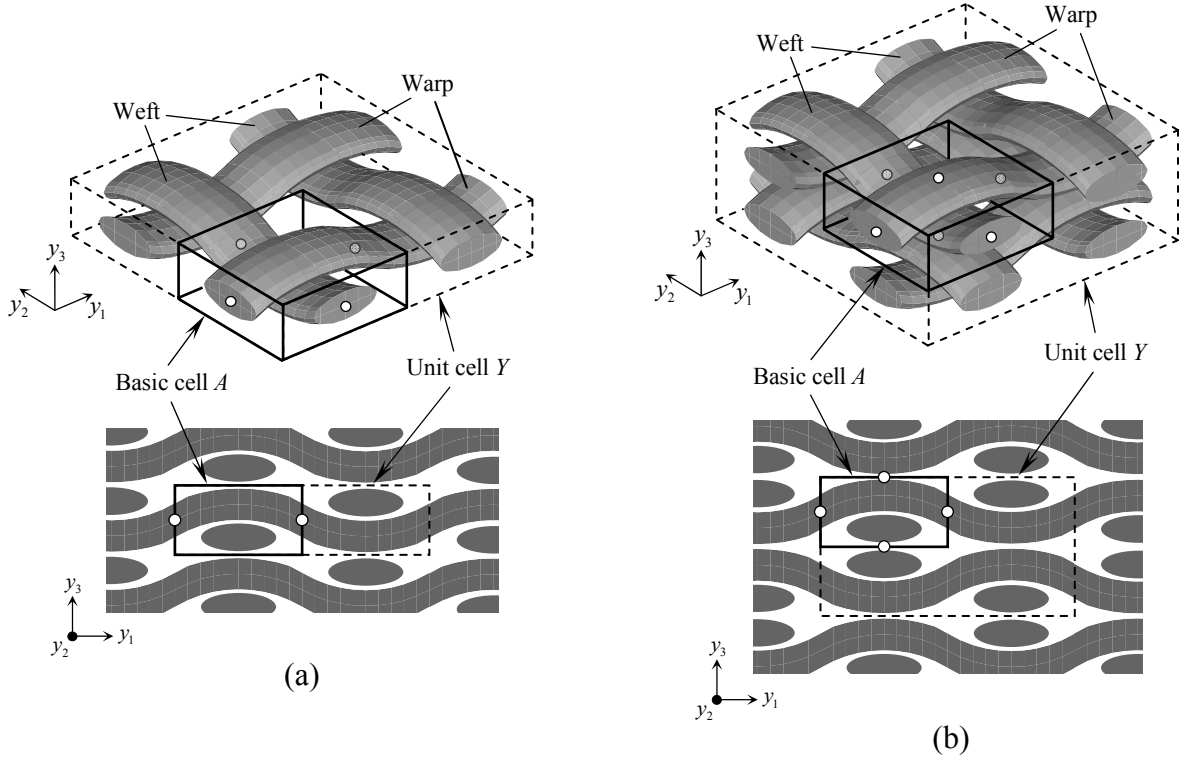


Fig. 2. Unit cells Y and basic cells A of plain-woven laminates; (a) in-phase, (b) out-of-phase.

to A in the y_3 -direction (stacking direction). The use of the point-symmetry and Y -periodicity of perturbed velocity as a boundary condition with our previous results [20-22] enables us to take A as the domain of analysis and to derive the boundary value problems Eqs. 5 and 6 as shown in section 3.

Next, with an out-of-phase laminate configuration, a unit cell Y is taken as indicated by the dashed lines in Fig. 2(b). The unit cell has two times the volume of an in-phase laminate configuration, but the same basic cell A is taken again as shown by the solid lines in Fig. 2(b). As indicated in the figure, the internal structure of laminate has the point-symmetry with respect to the centers of the top and bottom facets as well as lateral facets of A , i.e., the centers of all the boundary facets of A , which are denoted by the open circles in Fig. 2(b). Thus, the perturbed velocity in laminate distributes point-symmetrically with respect to these points. Employing the point-symmetric distribution of perturbed velocity as a boundary condition, we obtain the same boundary value problems Eqs. 5 and 6 as for an in-phase laminate configuration.

As mentioned above, we are able to derive the boundary value problems by taking the basic cell A as the domain of analysis for both the in-phase and out-of-phase laminate configurations. In

consequence, compared with the case of using unit cells, the domain of analysis is reduced to 1/4 and 1/8 for the in-phase and out-of-phase laminate configurations, respectively. The reduction of the domain of analysis leads to significantly less computational memory and time to solve the boundary value problems, which is of great use for the incremental analysis as dealt with in the present study.

3 Homogenization Theory

In this section, the homogenization theory of nonlinear time-dependent composites [18,19] is described by taking the basic cell A as the domain of analysis.

Let us consider that a plain-woven laminate is subjected to macroscopically uniform load and exhibits infinitesimal deformation both macroscopically and microscopically. The constituents of laminate are assumed to have elastic-viscoplastic properties and obey the following constitutive equation:

$$\dot{\sigma}_{ij} = c_{ijkl}(\dot{\epsilon}_{kl} - \beta_{kl}), \quad (1)$$

where $\dot{\sigma}_{ij}$ and $\dot{\epsilon}_{kl}$ indicate microscopic stress and strain rates, respectively, c_{ijkl} and β_{kl} signify elastic

stiffness and viscoplastic function, respectively, satisfying $c_{ijkl} = c_{jikl} = c_{ijlk} = c_{klij}$ and $\beta_{kl} = \beta_{lk}$. Then, the evolution equation of microscopic stress σ_{ij} , and the relationship between macroscopic stress rate $\dot{\Sigma}_{ij}$ and strain rate \dot{E}_{kl} are derived as follows [18,19]:

$$\dot{\sigma}_{ij} = c_{ijpq} (\delta_{pk} \delta_{ql} + \chi_{p,q}^{kl}) \dot{E}_{kl} - c_{ijkl} (\beta_{kl} - \varphi_{k,l}), \quad (2)$$

$$\dot{\Sigma}_{ij} = \langle c_{ijpq} (\delta_{pk} \delta_{ql} + \chi_{p,q}^{kl}) \rangle \dot{E}_{kl} - \langle c_{ijkl} (\beta_{kl} - \varphi_{k,l}) \rangle, \quad (3)$$

where δ_{ij} denotes Kronecker's delta, $(\cdot)_{,i}$ indicates the differentiation with respect to Cartesian coordinates y_i ($i=1, 2, 3$), and $\langle \cdot \rangle$ represents the volume average in A as

$$\langle \# \rangle = \frac{1}{|A|} \int_A \# dA. \quad (4)$$

Here, $|A|$ stands for the volume of A . Moreover, χ_i^{kl} and φ_i are the characteristic functions determined by solving the following boundary value problems:

$$\int_A c_{ijpq} \chi_{p,q}^{kl} v_{i,j} dA = - \int_A c_{ijkl} v_{i,j} dA, \quad (5)$$

$$\int_A c_{ijpq} \varphi_{p,q} v_{i,j} dA = \int_A c_{ijkl} \beta_{kl} v_{i,j} dA, \quad (6)$$

where v_i denotes an arbitrary velocity field satisfying the point-symmetry with respect to the centers of boundary facets of A or the Y -periodicity. The above problems are solved using FEM with the following boundary condition: With the in-phase laminate configuration, the point-symmetric condition with respect to the centers of lateral facets of A and the Y -periodic condition with respect to the top and bottom facets of A are imposed on χ_i^{kl} and φ_i . By contrast, with the out-of-phase laminate configuration, the point-symmetric condition with respect to the centers of all the boundary facets of A is imposed on χ_i^{kl} and φ_i .

4 Experimental Procedure

To verify the present method, in-plane uniaxial tensile tests of a plain-woven GFRP laminate at a constant strain rate were carried out at a room temperature. As illustrated in Fig. 3, coupon specimens were cut out from the plain-woven glass fiber/epoxy laminate (1000 mm \times 1000 mm, 10 plain fabrics stacked) manufactured by Nitto Shinko Corporation. Strain gauges and rectangular GFRP tabs were then attached on both sides of the

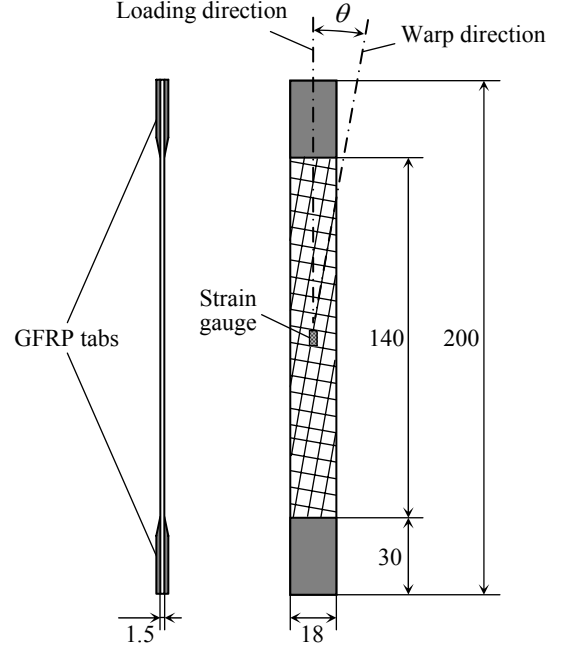


Fig. 3. Shape of specimens with dimensions in mm.

specimens. Regarding θ as the angle between the longitudinal direction (tensile direction) of specimens and the warp direction of plain fabrics, four kinds of θ were considered, i.e., $\theta = 0^\circ, 15^\circ, 30^\circ, 45^\circ$. The angle θ will be referred to as an off-axis angle hereafter, and $\theta = 0^\circ$ means on-axis loading. The tensile tests were done by a closed-loop servohydraulic testing machine with a load/strain computer controller. Strain rate was detected by the crosshead of testing machine, and the machine was controlled so that the specimens could be elongated at the constant strain rate 10^{-5} s^{-1} . It was confirmed by the strain gauges that the strain rate was kept precisely at 10^{-5} s^{-1} during the tests.

5 Analysis Condition

Using the present method, the in-plane elastic-viscoplastic and creep deformations of plain-woven glass fiber/epoxy laminates were analyzed under the macroscopic plane stress condition. In this section, the condition of the present analysis is described. The analysis was performed using VT64 Optron Workstation (AMD Optron 1.6 GHz) produced by Visual Technology, Inc.

5.1 Laminate Configuration and Loading Condition

For the elastic-viscoplastic analysis, the plain-woven GFRP laminates were assumed to have the

in-phase or out-of-phase laminate configuration. The loading condition is the same as the experiment: The laminates were subjected to in-plane uniaxial load and elongated at the constant strain rate 10^{-5}s^{-1} . Four kinds of off-axis angles, i.e., $\theta = 0^\circ, 15^\circ, 30^\circ, 45^\circ$, were considered. While, for the creep analysis, the laminates were assumed to have the in-phase laminate configuration, and subjected to a constant creep stress (80MPa) at the same four kinds of off-axis angles as in the elastic-viscoplastic analysis, i.e., $\theta = 0^\circ, 15^\circ, 30^\circ, 45^\circ$.

5.2 Basic Cell

In order to determine the geometry of basic cell, the microstructures of plain-woven GFRP laminate such as wavelength, shape and size of fiber bundles and volume fraction of fibers were investigated by the microscope observation of eight arbitrary aspects of the laminate from which the specimens had been cut out. Based on the average values of measurements, the basic cell was determined as illustrated in Fig. 4, and discretized into finite elements using eight-node isoparametric elements (1,624 elements, 1,995 nodes). This finite element mesh of basic cell corresponds to the meshes of unit cells with 6,496 and 12,992 elements for the in-phase and out-of-phase laminate configurations, respectively. The results of the present analysis were demonstrated to coincide with those of the analysis

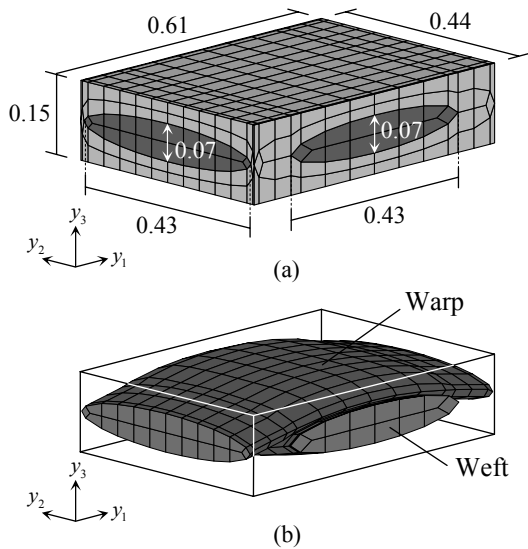


Fig. 4. Basic cell and finite element mesh; (a) full view with dimensions in mm, (b) fiber bundles in basic cell.

in which the basic cell was divided into 3,083 elements.

5.3 Material Properties

Fiber bundles were regarded as glass fiber/epoxy unidirectional composites and as linear elastic materials. The material properties of fiber bundles were calculated using the homogenization theory [11-13] on the assumption that the fiber volume fraction was 75 % in accordance with the microscope observation and that the bundles had a hexagonal fiber array. The elastic properties of glass fibers and epoxy used in the calculation are listed in Table 1. By contrast, the matrix (epoxy) was regarded as an isotropic elastic-viscoplastic material and to obey the following constitutive equation:

$$\dot{\epsilon}_{ij} = \frac{1 + \nu_m}{E_m} \dot{\sigma}_{ij} - \frac{\nu_m}{E_m} \dot{\sigma}_{kk} \delta_{ij} + \frac{3}{2} \dot{\epsilon}_0^p \left[\frac{\sigma_{eq}}{g(\bar{\epsilon}^p)} \right]^n \frac{s_{ij}}{\sigma_{eq}}, \quad (7)$$

where E_m , ν_m and n signify material constants, $g(\bar{\epsilon}^p)$ stands for the hardening function depending on equivalent viscoplastic strain $\bar{\epsilon}^p$, $\dot{\epsilon}_0^p$ indicates reference strain rate, s_{ij} denotes deviatoric part of σ_{ij} , and $\sigma_{eq} = \left[(3/2) s_{ij} s_{ij} \right]^{1/2}$. Incidentally, no failure was assumed to occur in the glass fibers and epoxy.

To identify the material constants and hardening function in Eq. 7, the tensile tests of plain-woven GFRP laminate were conducted with three kinds of strain rates. In the tests, 45° specimens were used because the viscoplastic behavior of epoxy matrix could be observed most clearly [20]. The relations between macroscopic stress Σ_θ and strain E_θ obtained from the tests are plotted in Fig. 5. The material constants and hardening function were then determined as shown in Table 1 so that the results of analysis in the case of $\theta = 45^\circ$ (in-phase laminate configuration) could reproduce the experimental data as accurately as possible. Incidentally, the above constitutive equation of

Table 1. Material constants.

Glass fiber	$E_f = 80 \times 10^3$	$\nu_f = 0.30$
Epoxy	$E_m = 5.0 \times 10^3$	$\nu_m = 0.35$ $\dot{\epsilon}_0^p = 10^{-5}$
	$n = 20$	$g(\bar{\epsilon}^p) = (\bar{\epsilon}^p)^{0.50} + 24.5/2.5^{\bar{\epsilon}^p}$

MPa (stress), mm/mm (strain), s (time).

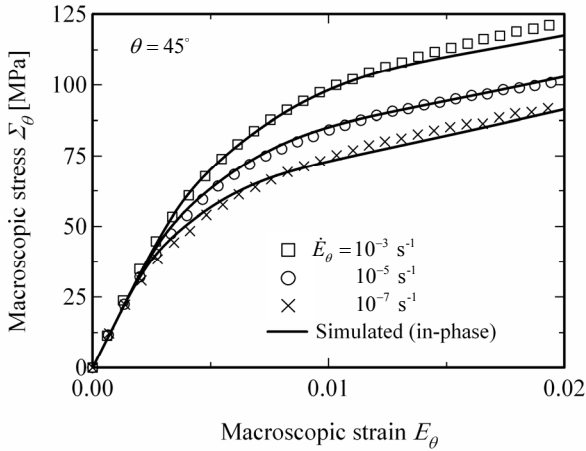


Fig. 5. Macroscopic tensile curves of plain-woven GFRP laminate with 45° off-axis angle at constant strain rates.

epoxy based on isotropic hardening is valid as far as monotonic loading is concerned [20,21].

6 Results of Analysis

6.1 Elastic-Viscoplastic Analysis

6.1.1 Macroscopic Behavior

The macroscopic stress-strain relations obtained from the present analysis and the tensile tests are shown in Fig. 6. The upper limits of strain, i.e., about 0.01 for $\theta = 0^\circ$ and 0.02 for $\theta = 15^\circ, 30^\circ, 45^\circ$, are taken to be relatively low compared with the fracture strains of specimens so that the influence of microscopic failures of fibers and matrix can be regarded as negligible. First, as seen from the experimental results indicated by the open circles in the figure, the almost linear behavior of plain-woven GFRP laminate is observed in the case of the on-axis loading ($\theta = 0^\circ$). By contrast, with off-axis loading, i.e., $\theta = 15^\circ, 30^\circ, 45^\circ$, the laminate exhibits considerable nonlinearity caused by the viscoplasticity of the matrix material. The viscoplastic flow stress suddenly decreases as θ increases, showing the marked in-plane anisotropy of laminate [6,8]. Comparing such experimental data with the results of the present analysis indicated by the lines in Fig. 6, it is found that the present method is successful in predicting the macroscopic behavior of plain-woven GFRP laminate.

Next, we compare the results of in-phase laminate configuration (solid lines) with those of the out-of-phase one (dashed lines). As seen from Fig. 6, the differences between both the results are not

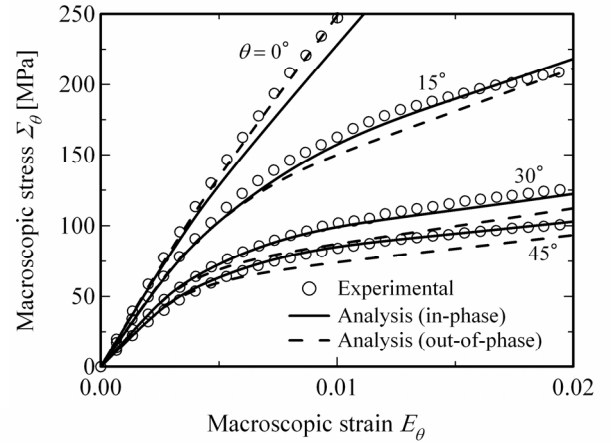


Fig. 6. Macroscopic stress versus strain relations of plain-woven GFRP laminates at $\dot{E}_\theta = 10^{-5} \text{ s}^{-1}$.

observed in the elastic but rather in the viscoplastic region; the differences of viscoplastic flow stresses reach 5~15% at $E_\theta = 0.01$. A closer look at the figure reveals that, with on-axis loading ($\theta = 0^\circ$), the flow stress of the out-of-phase laminate configuration is higher than that of the in-phase one, whereas in off-axis loading ($\theta = 15^\circ, 30^\circ, 45^\circ$), the relation is reversed, an issue to be discussed in more detail in the next section. It is thus shown that the laminate configurations of plain fabrics affect the viscoplastic, not the elastic, behavior of plain-woven GFRP laminates. Moreover, the laminate configurations of plain fabrics reportedly affected the microscopic failure behavior of plain-woven laminates subjected to in-plane on-axis load [14,17,24].

6.1.2 Microscopic Behavior

To determine why the flow stress varied depending on the laminate configurations, we first examined the deformations of a cross section of the basic cell and the distributions of microscopic equivalent stress in the case of $\theta = 0^\circ$ (Fig. 7). In the figure, the displacement is magnified 10 times. In the in-phase laminate configuration, the laminate exhibits marked out-of-plane deformation [17], whereas such out-of-plane deformation disappears with the out-of-phase laminate configuration because of the symmetry of internal structure, resulting in a large interaction between adjacent warps. The interaction, moreover, causes more stress in the warp of the out-of-phase laminate configuration higher than the in-phase one as shown in Fig. 7. In consequence, the viscoplastic flow

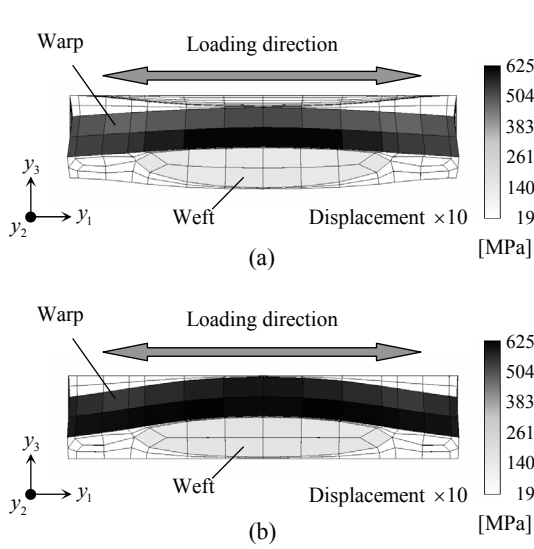


Fig. 7. Distributions of equivalent stress in basic cells at $E_\theta = 0.01$ ($\theta = 0^\circ$); (a) in-phase, (b) out-of-phase.

stress of the out-of-phase laminate configuration became higher than that in the in-phase one as mentioned in the previous section (see Fig. 6).

Next, we discuss the distributions of resultant shear stress at the top facet of the basic cell in the case of $\theta = 45^\circ$ (Fig. 8). In the figure, the magnitudes of vectors signify $[(\sigma_{23})^2 + (\sigma_{31})^2]^{1/2}$. As seen from Fig. 8(a), considerable shear stress takes place in the case of the in-phase laminate configuration because the adjacent warp and weft rotate in opposite directions, respectively, due to the 45° off-axis loading (Fig. 9(a)). By contrast, in the case of the out-of-phase laminate configuration, such shear stress is hardly observed (Fig. 8(b)) because the adjacent warps rotate in the same direction (Fig. 9(b)). As a result, the viscoplastic flow stress of the in-phase laminate configuration became higher than that of the out-of-phase one as shown in Fig. 6. The same tendency was found at the bottom facet of the basic cell, where there was the remarkable shear stress of the in-phase laminate configuration and little shear stress of the out-of-phase one.

6.2 Creep Analysis

Figure 10 shows the macroscopic creep curves of the plain-woven GFRP laminates at a constant creep stress, 80MPa, with four kinds of off-axis angles, $\theta = 0^\circ, 15^\circ, 30^\circ, 45^\circ$. First, it is seen from the figure that creep strain is hardly observed at $\theta = 0^\circ$ (on-axis loading). Similarly, considerably small creep strain occurs at $\theta = 15^\circ$.

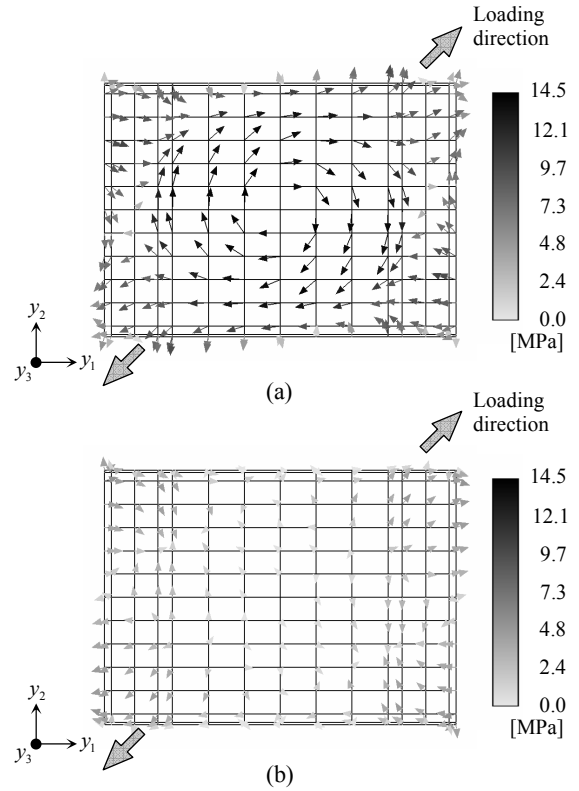


Fig. 8. Distributions of resultant shear stress $[(\sigma_{23})^2 + (\sigma_{31})^2]^{1/2}$ on top facets of basic cells at $E_\theta = 0.02$ ($\theta = 45^\circ$); (a) in-phase, (b) out-of-phase.

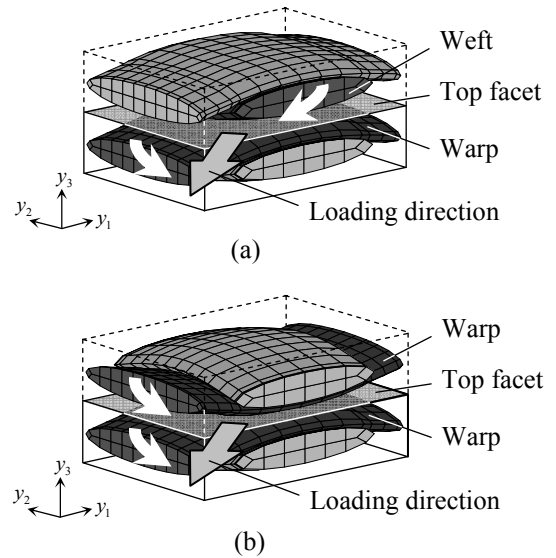


Fig. 9. Rotation of fiber bundles around top facets of basic cells under off-axis loading; (a) in-phase, (b) out-of-phase.

But, with $\theta = 30^\circ$, the creep strain suddenly increases and reaches more than five times the creep

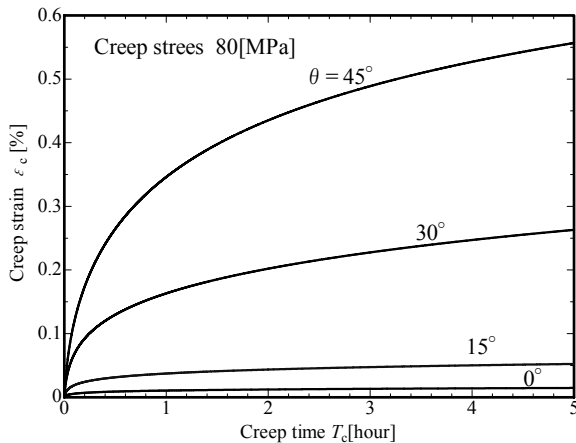


Fig. 10. Macroscopic off-axis creep behavior of plain-woven GFRP laminates at constant creep stress (80MPa).

strain for $\theta = 15^\circ$. The creep strain further increases at $\theta = 45^\circ$, and becomes over twice higher than that at $\theta = 30^\circ$. These results suggest that the plain-woven GFRP laminates have marked in-plane anisotropy with respect to macroscopic creep behavior.

7 Conclusions

In this study, first, the basic cell was introduced into the homogenization analysis of plain-woven laminates as the domain of analysis by utilizing the point-symmetry of internal structures of laminates with the in- and out-of-phase laminate configurations. The basic cell enabled us to reduce the domain of analysis to 1/4 and 1/8 with respect to the in- and out-of-phase laminate configurations, respectively, in comparison with the case of using unit cells. Next, the time-dependent homogenization theory was reconstructed for the basic cell. The present method was then applied to the in-plane elastic-viscoplastic and creep analysis of plain-woven GFRP laminates. Moreover, the uniaxial tensile tests of a plain-woven GFRP laminate at a constant strain rate were carried out at a room temperature. It was thus demonstrated that the experimental results were accurately predicted by the present analysis. It is also shown that the plain-woven GFRP laminates exhibit marked in-plane anisotropy with respect to the elastic-viscoplastic and creep behaviors.

Acknowledgement

The support in part by the Ministry of Education, Culture, Sports, Science and Technology, (No. 18760075) is acknowledged.

References

- [1] Tan P., Tong L. and Steven GP. "Modelling for predicting the mechanical properties of textile composites – A review". *Compos Part A*, Vol. 28, pp 903-22, 1997.
- [2] Quek SC., Waas AM., Shahwan KW. and Agaram V. "Analysis of 2D triaxial flat braided textile composites". *Int J Mech Sci*, Vol. 45, pp 1077-96, 2003.
- [3] Ishikawa T. and Chou TW. "One-dimensional micromechanical analysis of woven fabric composites". *AIAA J*, Vol. 21, pp 1714-21, 1983.
- [4] Guedes JM. and Kikuchi N. "Preprocessing and postprocessing for materials based on the homogenization method with adaptive finite element methods". *Comput Methods Appl Mech Eng*, Vol. 83, pp 143-98, 1990.
- [5] Naik NK. and Ganesh VK. "Prediction of on-axes elastic properties of plain weave fabric composites". *Compos Sci Technol*, Vol. 45, pp 135-52, 1992.
- [6] Fujii T., Amijima S. and Lin F. "Study on strength and nonlinear stress-strain response of plain woven glass fiber laminates under biaxial loading". *J Compos Mater*, Vol. 26, pp 2493-510, 1992.
- [7] Uetsuji Y. and Zako M. "Damage analysis of woven fabric composite materials". *Zairyo*, Vol. 48, pp 1029-34, 1999. (in Japanese).
- [8] Carvelli V. and Poggi C. "A homogenization procedure for the numerical analysis of woven fabric composites". *Compos Part A*, Vol. 32, pp 1425-32, 2001.
- [9] Osada T., Nakai A. and Hamada H. "Initial fracture behavior of satin woven fabric composites". *Compos Struct*, Vol. 61, pp 333-9, 2003.
- [10] Zako M., Uetsuji Y. and Kurashiki T. "Finite element analysis of damaged woven fabric composite materials". *Compos Sci Technol*, Vol. 63, pp 507-16, 2003.
- [11] Bensoussan A. and Lions JL. and Papanicolaou G. "Asymptotic analysis for periodic structures". North-Holland Publishing Company, 1978.
- [12] Sanchez-Palencia E. "Non-homogeneous media and vibration theory, Lecture notes in physics, No. 127". Springer-Verlag, 1980.
- [13] Bakhvalov N. and Panasenko G. "Homogenisation: Averaging processes in periodic media". Kluwer Academic Publishers, 1984.
- [14] Takano N., Zako M. and Sakata S. "Three-dimensional microstructural design of woven fabric

**OFF-AXIS VISCOPLASTIC BEHAVIOR OF PLAIN-WOVEN LAMINATES:
ANALYSIS USING TIME-DEPENDENT HOMOGENIZATION THEORY**

- composite materials by the homogenization method: 1st report, Effect of mismatched lay-up of woven fabrics on the strength". *Trans Jpn Soc Mech Eng, Ser A*, Vol. 61, pp 1038-43, 1995. (in Japanese).
- [15] Takano N., Uetsuji Y., Kashiwagi Y. and Zako M. "Hierarchical modelling of textile composite materials and structures by the homogenization method". *Model Simul Mater Sci Eng*, Vol. 7, pp 207-31, 1999.
- [16] Whitcomb J. and Srirengan K. "Effect of various approximations on predicted progressive failure in plain weave composites". *Compos Struct*, Vol. 34, pp 13-20, 1996.
- [17] Uetsuji Y., Ishiwari Y., Zako M. and Kurashiki T. "Verpoest I. Effect of mismatch of stacking phase on damage development of plain woven fabric composite materials". *Zairyo*, Vol. 53, pp 403-9, 2004. (in Japanese).
- [18] Wu X. and Ohno N. "A homogenization theory for time-dependent nonlinear composites with periodic internal structures". *Int J Solids Struct*, Vol. 36, pp 4991-5012, 1999.
- [19] Ohno N., Wu X. and Matsuda T. "Homogenized properties of elastic-viscoplastic composites with periodic internal structures". *Int J Mech Sci*, Vol. 42, pp 1519-36, 2000.
- [20] Matsuda T., Ohno N., Tanaka H. and Shimizu T. "Homogenized in-plane elastic-viscoplastic behavior of long fiber-reinforced laminates". *JSME Int J, Ser A*, Vol. 45, pp 538-44, 2002.
- [21] Matsuda T., Ohno N., Tanaka H. and Shimizu T. "Effects of fiber distribution on elastic-viscoplastic behavior of long fiber-reinforced laminates". *Int J Mech Sci*, Vol. 45, pp 1583-98, 2003.
- [22] Ohno N., Matsuda T. and Wu X. "A homogenization theory for elastic-viscoplastic composites with point symmetry of internal distribution". *Int J Solids Struct*, Vol. 38, pp 2867-78, 2001.
- [23] Ganesh VK. and Naik NK. "Failure behaviour of plain weave fabric laminates under in-plane shear loading: effect of fabric geometry". *Compos Struct*, Vol. 30, pp 179-92, 1995.
- [24] Le Page BH., Guild FJ., Ogin SL. and Smith PA. "Finite element simulation of woven fabric composites". *Compos Part A*, Vol. 35, pp 861-72, 2004.
- [25] Zeman J. and Šejnoha M. "Homogenization of balanced plain weave composites with imperfect microstructure: Part I – Theoretical formulation". *Int J Solids Struct*, Vol. 41, pp 6549-71, 2004.